Chain model of a magnetorheological suspension in a rotating field

Sonia Melle
Instituto de Microelecronica de Madrid, CSIC, Isaac Newton 8 (PTM) Tres Cantos, 28760 Madrid, Spain

James E. Martin
Sandia National Laboratories, Albuquerque, New Mexico 87185-1421

We develop an athermal chain model for magnetorheological suspensions in rotating magnetic fields. This model is based on a balance of hydrodynamic and magnetostatic forces and focuses on the mechanical stability of chains. Using a linear approximation of the chain shape, we compute the orientation and size of a critical chain in a rotating magnetic field as a function of the Mason number Mn, which is the ratio of dipolar to hydrodynamic forces between two particles in contact. The critical chain length is found to scale with the inverse square root of Mn, and its orientation relative to the instantaneous field is independent of Mn. The actual nonlinear shape of a chain in a rotating field is then computed self-consistently. Finally, the effect of local fields on the dipolar interaction force is considered, leading to predictions for the chain shape and orientation that depend rather strongly on the magnetic permeability of the particles. A principal finding is the possibility of brittle or ductile chain fracture, depending on the permeability of the particles. Single-chain simulations confirm this prediction, as do experimental measurements. © *2003 American Institute of Physics.*
[DOI: 10.1063/1.1570817]

I. INTRODUCTION

Magnetorheological (MR) suspensions consist of magnetically soft particles in a nonmagnetic fluid. These fluids are useful in electromechanical devices as damping fluids with field-controllable rheology, but can also be considered a model system for the study of structure formation and dynamics in dipolar suspensions with tunable particle interactions. We have recently reported studies of the dynamics of MR suspensions in low-frequency rotating magnetic fields ($f = \omega/2\pi < 10$ Hz). In these experiments the magnetic interactions between particles greatly exceed the thermal force, so Brownian motion does not play a significant role.[1–5]

Upon applying a rotating field to a dilute suspension, particle chains quickly form, aggregating and fragmenting until a steady state is attained.[3,5] In a reference frame rotating with a field, the behavior of a single chain is similar to the problem of a chain in a stationary magnetic field subjected to simple shear flow, with the fluid flow normal to the magnetic field. However, in a rotating field the chains rotate like propellers, causing significant chain–chain interference effects that do not exist in simple shear flow. In either case there are two forces acting on the particles: a largely dipolar magnetic force that tends toward chain formation and a viscous drag that tends toward fragmentation. The chain statistics of such a system in steady state depend only on the Mason number Mn, a dimensionless ratio of the viscous forces to the dipolar forces. Chainlike structures form when $Mn \ll 1$.

Previous work on the behavior of colloidal suspensions in rotating fields show that there are two regimes of behavior: a low-frequency regime, where chains rotate with the field, and a high-frequency regime, where chains are no longer stable and two-dimensional aggregates form. Helgesen *et al.* studied mechanically bound pairs of magnetic holes[6,7] (nonmagnetic particles in a ferrofluid) under rotating magnetic fields and found synchronous and nonsynchronous regimes depending on the driving frequency. Halsey *et al.*[8] reported on the formation of two-dimensional aggregates in high-frequency electric fields, and Martin *et al.*[9,10] used high-frequency magnetic fields to create sheetlike, layered particle composites with enhanced magnetic properties.

Our interest is in the low-frequency regime, where particle chains form that rotate at the frequency of the applied field. As in the case of simple shear,[11] where it has been demonstrated that chains aggregate to a longer average size and fragment to a shorter size in response to decreasing or increasing shear rates, we have found that chains aggregate and fragment in response to decreasing or increasing field frequency,[3] the average size of the structures scaling as the inverse square root of Mn. Scattering dichroism experiments[1,2] show that particle structures lag the field by a phase angle that increases with increasing rotating field frequency, though this increase appears to be due to the formation of nonlinear particle aggregates at large frequencies.[4]

II. THEORY

A. Mason number

The dipolar force results from particle polarization in the magnetic field. The dipole moment of a single particle in an applied magnetic field $\mathbf{H}_0$ is given by $\mathbf{m} = v\chi_p\mathbf{H}_0$, where a is the particle radius, χ_p is the particle susceptibility, and $v = 4\pi a^3/3$ is the particle volume. In general, the shape of a particle creates a demagnetizing field that opposes the field attempting to polarize it, vastly reducing the susceptibility of a particle relative to the susceptibility of the material of which it is composed. For a spherical particle the so-called

9875

demagnetizing factor is 1/3, leading to a particle susceptibility of $\chi_p = 3\beta$ where $\beta = (\mu_p - \mu_c)/(\mu_p + 2\mu_c)$ is the magnetic permeability contrast factor.[11–13] In this expression, μ_p is the magnetic permeability of the material of which the particles are composed and μ_c is the permeability of the continuous liquid phase. In terms of the particle magnetization $M_p = m/v$ the *attractive* dipolar force between two contacting field-aligned particles is $f_d \sim \mu_0 \mu_c a^2 M_p^2$, where the vacuum permeability is $\mu_0 = 4\pi \times 10^{-7}$ Tm/A.

The Stokes drag on a particle is $6\pi\eta a(\mathbf{v}_f - \mathbf{v}_p)$ in terms of the velocity of the fluid $\mathbf{v}_f$ at the particle center of mass, the particle velocity $\mathbf{v}_p$, and the liquid viscosity η. A single particle not acted on by a body force will move with the fluid (after a brief acceleration) and experience zero Stokes drag, but two particles held together by dipolar forces will experience a Stokes drag because it is their center of mass that moves with the fluid. In a rotating magnetic field in a stationary fluid, the contacting particles will rotate at an angular velocity ω, so each particle will move at a velocity of magnitude $a\omega$, generating a hydrodynamic drag force $f_h \sim a^2 \eta \omega$.

If the hydrodynamic force is smaller than the dipolar force, then one can expect the dimer to be stable. The Mason number Mn is the dimensionless parameter that compares these forces. For shear flow, this number has been defined with different proportionality factors.[11,14–17] To facilitate comparison with the chain model for electro- and magnetorheology[11] we define the Mason number as

$$Mn = \frac{\eta\omega}{2\mu_0\mu_c\beta^2 H_0^2}. \qquad (1)$$

In experimental work on rotating magnetic fields we have used a different definition: the relation between these is $Mn' = 32Mn$.

B. Critical chain angle

We first consider the elementary problem of two contacting polarizable particles of radius a in an external field $\mathbf{H}_0$ applied along the z axis. Each of these particles is acted on by equal and opposite applied forces of magnitude f_a, which in general cause the contacting pair to be misaligned with the field. We seek to understand the effect of this applied force on the alignment and stability of this dipole pair, and we will compute this in the so-called fixed point dipole approximation, wherein each particle is polarized by the applied field alone: i.e., $\mathbf{m} = v3\beta\mathbf{H}_0$. Later we will consider the effect of local fields on particle polarization.

In the fixed point dipole approximation, the dipole moment $\mathbf{m}$ on each of these particles is aligned with the z axis, creating a dipole field $\mathbf{H}_m = (m/4\pi r^3)(2\cos\theta\hat{\mathbf{r}} + \sin\theta\hat{\boldsymbol{\theta}})$, where θ is the angle from the z axis. Each dipole feels the applied field plus this dipole field. The general expression for the magnetic force on a dipole is $\mathbf{F} = \mu_0\mu_c\mathbf{m}\cdot(\nabla\mathbf{H})$, which gives the *attractive dipole interaction* force (note the sign convention)

$$\mathbf{f}_d = f_c[(3\cos^2\theta - 1)\hat{\mathbf{r}} + \sin2\theta\hat{\boldsymbol{\theta}}]. \qquad (2)$$

The prefactor is the contact force $f_c = (3\pi/4)\mu_0\mu_c a^2 \beta^2 H_0^2$, which in terms of the Mason number Mn is $3\pi a^2 \eta\omega/8Mn$.

It is worth noting that the application of an electric field is completely analogous, but slightly more complex due to the possibility of charge conduction. At high frequencies the contact force $f_c = (3\pi/4)\epsilon_0\epsilon_c a^2 \beta^2 E_0^2$ is due to dielectric contrast, whereas at low frequencies conductivity contrast becomes dominant.[18] At the theoretical level of self-consistent point dipoles there is no further difference between the study of electrorheological (ER) and MR fluids, so once a theory is expressed in terms of the relevant Mason number, it applies equally to both types of fluids.

The external force vector makes an angle ϕ to the z axis. The force can be resolved into components parallel and perpendicular to the chain, $\mathbf{f}_a = \cos(\phi - \theta)f_a\hat{\mathbf{r}} + \sin(\phi - \theta)f_a\hat{\boldsymbol{\theta}}$. The angle the pair makes to the field is computed by balancing the tangential component of the attractive dipole force to that of the applied force, $\mathbf{f}_a\cdot\hat{\boldsymbol{\theta}} = \mathbf{f}_d\cdot\hat{\boldsymbol{\theta}}$. This gives

$$\frac{\sin 2\theta}{\sin(\phi - \theta)} = \frac{f_a}{f_c}. \qquad (3)$$

For the pair to remain in contact, the radial component of the dipole force must dominate the radial component of the applied force, $\mathbf{f}_d\cdot\hat{\mathbf{r}} \geq \mathbf{f}_a\cdot\hat{\mathbf{r}}$, or

$$\frac{3\cos^2\theta - 1}{\cos(\phi - \theta)} \geq \frac{f_a}{f_c}. \qquad (4)$$

The critical stability angle θ_c obtains when these forces are equal and can be obtained by combining this result with Eq. (3):

$$\frac{3\cos^2\theta_c - 1}{\cos(\phi - \theta_c)} = \frac{\sin 2\theta_c}{\sin(\phi - \theta_c)}. \qquad (5)$$

The critical angle depends only on the direction of the applied force.

Consider the case where dipole pair is at the center of a long, linear chain of identical dipoles subjected to some type of fluid flow (the actual shape of a chain is treated below). The applied force on the central pair is a sum of the hydrodynamic forces on all of the dipoles, including the pair itself.

C. Simple shear

First, consider the case of simple shear with the fluid flow normal to the field. Because the hydrodynamic drag at each particle is normal to the field, $\phi = \pi/2$. Substituting this into Eq. (5) gives $3\cos^2\theta_c - 1 = 2\sin^2\theta_c$ so $\cos\theta_c = \sqrt{3/5}$. This gives a maximum chain angle of $\sim 39.23°$, which is a well-known prediction[11] for standard electro- and magnetorheology. In fact, this result is actually independent of the assumption of chain linearity, since regardless of the chain shape the hydrodynamic drag on each particle is parallel.

D. Rotating field

The simple shear case can be contrasted with that of a rotating field. In a rotating reference frame with the field along the z axis the chain appears to be in vortex flow. The hydrodynamic drag vectors are then in the direction $\phi = \theta$

$+\pi/2$ and, from Eq. (5), $3\cos^2\theta_c-1=0$, so $\cos\theta_c=\sqrt{1/3}$. The maximum chain angle is apparently $\sim54.7°$, which is an entirely trivial result: this is simply the angle where the radial component of the dipolar force vanishes [Eq. (2)]. In fact, this problem is subtle for two reasons. First, this result depends on the assumption of chain linearity, because for nonlinear chains the drag forces are not parallel. Second, this chain angle does not correspond to a stationary state, a point that requires further consideration.

For a linear chain the tangential hydrodynamic force on the central pair of particles is just f_a, and the magnitude of this force depends only on the chain length, not the chain angle θ. The tangential component of the dipolar force between these particles depends on chain angle through $f_c\sin2\theta$ and has a maximum at 45°, at which point the derivative of this force with respect to θ changes sign. This angle is thus the limit of chain stability, defined here as a stationary state, because a chain that grows long enough to rotate to 45° will rotate to $\sim54.7°$ and fragment. A chain that is somehow created, and has a perfect torque balance, within this interval of $45°<\theta<54.7°$ will be unstable to noise. A fluctuation to slightly larger angles will cause the hydrodynamic torque to dominate the dipolar torque, and the chain will rotate to 54.7° and fragment. A fluctuation to slightly smaller angles will cause the dipolar torque to dominate the hydrodynamic, and the chain will rotate to an angle equally beneath 45°, where it will be stationary, but metastable.

The region of metastability is from $45°-9.7°=35.3°$ to 45°. A stationary chain with a torque balance in this region could in principle experience a fluctuation past the complementary angle, where it would immediately rotate further and fragment. The angle of 35.3° is thus the upper limit of stability and 45° is the limit of metastability. (The issue of the lifetime of a thermal chain is beyond the scope of the paper, but has been examined for the case of steady shear.[19]) Bear in mind that accounting for local field effects (below) will change these angles, though the concept remains.

E. Critical Mason number

It is now straightforward to determine the Mason number Mn^* above which a dimer becomes metastable. For a dimer the applied force is due to the hydrodynamic drag on the particles themselves, $f_a=6\pi\eta a^2\omega$. Substituting this into Eq. (3) and using $\phi=\theta+\pi/2$ gives $Mn^*=\frac{1}{16}\sin(2\theta_c)$ $=1/(12\sqrt{2})$. At larger Mason numbers chains are metastable. The upper limit of metastability occurs when $\sin(2\theta)=1$ or $Mn^{**}=1/16$.

F. Chain length

To compute the dependence of the chain length on the field rotation frequency ω we label the particles from $-N$ to N, with particle zero at the chain center, which is at the origin. In the rotating reference frame the fluid velocity is $\mathbf{v}_f=\omega r\hat{\boldsymbol{\theta}}$. For a stationary chain (constant phase lag behind the field) the hydrodynamic drag on the ith particle is $\mathbf{f}_{h,i}$ $=12\pi\eta a^2\omega i\hat{\boldsymbol{\theta}}$. Because this force is perpendicular to the chain, it creates zero tension, but it does create a torque in

the chain. The torque acting on particles i and $i+1$ is a sum over contributions from all particles further out in the chain:

$$S_i=\sum_{k=i+1}^{N}\mathbf{f}_{h,i}\cdot\hat{\boldsymbol{\theta}}\cong6\pi\eta a^2\omega(N^2-i^2).\qquad(6)$$

This is a maximum at the chain center, where the applied force is $\mathbf{f}_a=S_0\hat{\boldsymbol{\theta}}=6\pi\eta\omega a^2N^2\hat{\boldsymbol{\theta}}$. For a chain of $2N+1$ particles the chain angle is computed by balancing this torque against the tangential component of the dipole force, $\mathbf{f}_d\cdot\hat{\boldsymbol{\theta}}$ $=f_c\sin2\theta$, to obtain

$$\sin2\theta=16MnN^2.\qquad(7)$$

This result is valid if the chain is at least metastable. As we have seen, this occurs when $\sin2\theta=(2/3)\sqrt{2}$ or when

$$(2N^*)^2=\frac{1}{3\sqrt{2}Mn}.\qquad(8)$$

The physical picture is simple: a dilute solution of polarizable particles in a rotating field will form chains. These chains will grow, and their angle relative to the field will grow essentially quadratically with their length until a critical angle is achieved that is independent of Mn. Chains at this critical angle will have a length that depends on the inverse square root of Mn. This general description is exactly that obtained for simple shear,[10] though the details differ. Note also that although we have always taken the large-N limit in the summations, substituting $N^*=1$ into Eq. (8) gives a value of the Mason number exactly equal to the critical Mason number Mn^*. Equation (8) should thus be interpreted as being correct for chains of $2N^*$ particles, not $2N^*+1$ particles.

G. Chain interference

Chains in a rotating field whirl like propellers, causing interference effects. Here we will give a rough estimate of the limit of the dilute concentration regime where such effects can be ignored. We first note that a chain will tend to rotate in the plane swept out by the field. Thus we consider chain interference in a thin volume of thickness $d=2a$. The area swept out by a rotating chain is $A_s=(\pi/4)L^2$ $=(\pi/4)N_{tot}^2d^2$, where L is the chain length and N_{tot} is the total number of particles in the chain. The volume of chain within this area is $V_{chain}=(\pi/6)d^3N_{tot}$, and dividing this by the volume A_sd of the slab gives a volume fraction of particles within the swept volume of $\phi_s=2/(3N_{tot})$. When this volume fraction exceeds the overall volume fraction ϕ of particles one can expect strong chain interference effects. From Eq. (7) we see that the dilute concentration regime is attained only when the condition $Mn\gg\phi^2$ is satisfied.

H. Chain shape

The shape of a chain in a rotating field can be computed from a continuous balance of forces along its length. The definition of variables is given in Fig. 1, the important point being that each particle has its own phase lag angle ϕ_i to the applied field, so in the rotating reference frame the fluid velocities are no longer parallel, with $\mathbf{v}_{f,i}=\omega r_i\hat{\boldsymbol{\phi}}_i$. Note also
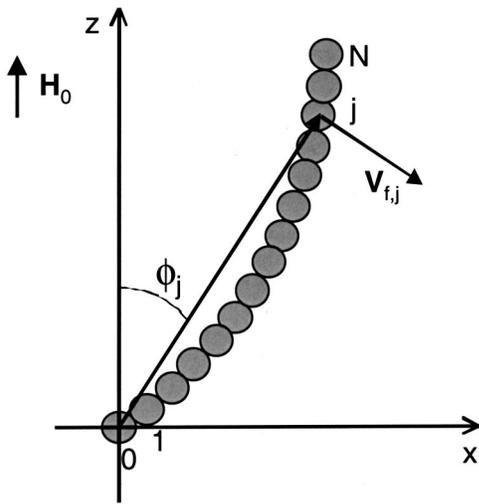
FIG. 1. Coordinates for the computation of the chain shape. The fluid velocity vector at particle j is normal to the vector ϕ_j.
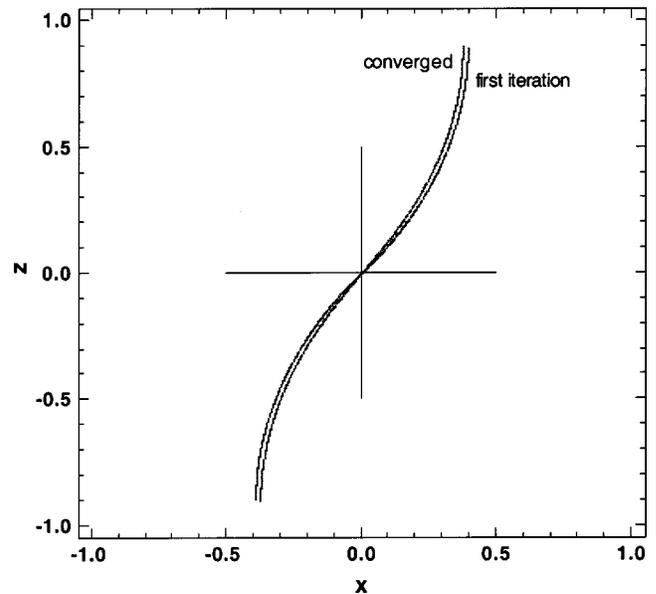

FIG. 2. The fully converged chain shape in the fixed point dipole approximation is compared to the first iteration. The most notable difference is the decreased critical chain angle. In this figure the applied field is rotating counterclockwise and at this instant is in the z direction.

that the angle θ_i that the line of centers between particles i-1 and i makes to the field direction also depends on the position in the chain. The hydrodynamically induced torque in the chain is given by $S_i = \Sigma_{k=i}^N \mathbf{f}_{h,k} \cdot \hat{\boldsymbol{\theta}}_i$. Using $\mathbf{f}_{h,k} = 6\pi\eta a \mathbf{v}_{f,i}$ and balancing this torque against the tangential dipolar force gives

$$\sin 2\theta_i = 32Mn\hat{\boldsymbol{\theta}}_i \cdot \sum_{k=i}^N \left(\frac{r_k}{2a}\right)\hat{\boldsymbol{\phi}}_k, \tag{9}$$

where $\hat{\boldsymbol{\theta}}_i \cdot \hat{\boldsymbol{\phi}}_k = \cos\theta_i\cos\phi_k + \sin\phi_i\sin\phi_k$. The hydrodynamically induced tension in the chain is given by $T_i = \Sigma_{k=i}^N \mathbf{f}_{h,k} \cdot \Delta\hat{\mathbf{r}}_i$ where the bond vector $\Delta\hat{\mathbf{r}}_i = \mathbf{r}_i - \mathbf{r}_{i-1}$, and balancing this against the radial dipolar force gives

$$3\cos^2\theta_i - 1 \geqslant 32Mn\Delta\hat{\mathbf{r}}_i \cdot \sum_{k=i}^N \left(\frac{r_k}{2a}\right)\hat{\boldsymbol{\phi}}_k, \tag{10}$$

with $\Delta\hat{\mathbf{r}}_i \cdot \hat{\boldsymbol{\phi}}_k = \sin\theta_i\cos\phi_k - \cos\theta_i\sin\phi_k$. Now define the sums $\Psi_i = N^{-2}\Sigma_{k=i}^N (r_k/2a)\cos\phi_k$ and $\Omega_i = N^{-2}\Sigma_{k=i}^N (r_k/2a)\sin\phi_k$ which for large N are independent of N and a. Substituting these into Eqs. (9) and (10) results in the coupled equations

$$\sin 2\theta_i = \alpha A, \tag{11a}$$

$$3\cos^2\theta_i - 1 \geqslant + \alpha B, \tag{11b}$$

where $\alpha = 32MnN^2$, $A = \Psi_i\cos\theta_i + \Omega_i\sin\theta_i$, and $B = \Psi_i\sin\theta_i - \Omega_i\cos\theta_i$.

An approximate solution to these coupled equations can be found from an iterative procedure. First, we guess a zeroth-order solution with $\theta_i = \phi_i = 45°$, which gives $\Psi_i = \Omega_i = 1/(2\sqrt{2})$. Noting that $\sin 2\theta_1 = 1$ and $\cos\theta_1 = \sin\theta_1 = 1/\sqrt{2}$, we can determine from Eq. (11a) that $\alpha = 2$ or $16MnN^2 = 1$. With this result for α an improved estimate for the angles along the chain can be obtained from Eq. (11a), setting $\cos\theta_i = \sin\theta_i = 1/\sqrt{2}$ on the right-hand side. For large N the sums Ψ_i and Ω_i are easily evaluated, with the result $A = (1 - \sigma^2)/2$, where $\sigma = iN$ is the contour variable of the

chain. Equation (11b) is immediately satisfied because $B = 0$ (in a linear chain there is no tension). To first order,

$$\sin 2\theta = \sin 2\theta_0(1 - \sigma^2), \tag{12}$$

where $\sin 2\theta_0 = 16MnN^2$. In fact, this solution is that previously derived[10] for a chain in simple shear, though the central chain angle is somewhat different.

To find self-consistently the shape of a critical chain we continue to iterate, but we must now take into account the stability conditions, Eq. (11b), because the first-order chain shape is nonlinear and the hydrodynamic tension is nonzero. The terms A and B can be computed from the first-order result for the chain angles, Eq. (12), with the first-order chain coordinates $\mathbf{r}_k/2a = \Sigma_{i=1}^k \sin\theta_i\hat{\mathbf{x}} + \cos\theta_i\hat{\mathbf{z}}$. Then the central chain angle can be found from $(3\cos^2\theta_0 - 1)/\sin 2\theta_0 = B/A$. This angle can then be used to find α through the relation $\alpha = \sin 2\theta_0/A$, and the second-order chain angles can be computed from $\sin 2\theta_i = \alpha A$. This process can be repeated to convergence, but is actually almost quantitative after a couple of cycles.

In Fig. 2 the fully converged chain shape is compared to the first-order approximation. This is, of course, the shape of a critical chain that is at the limit of stability. The angle of the chain at the center converges to 38.37°, the average chain angle is 22.5°, and $\alpha = 1.991$. Note that in this figure the field and chain are rotating counterclockwise. Plotting the chain angle against the contour length is more revealing of the difference between the first-order approximation and the converged result, Fig. 3.
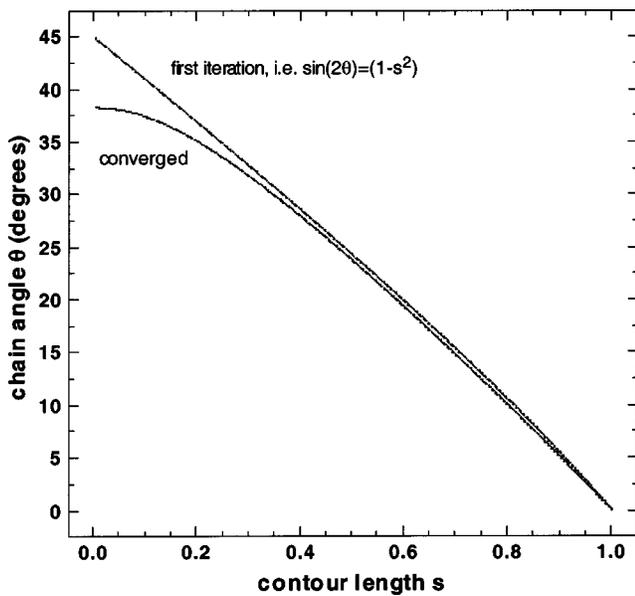
FIG. 3. The difference between the fully converged chain angle and that of the first iteration is more obvious when plotted against contour length.

I. Improvement to the basic model

The basic model successfully captures the qualitative features of particle chains in rotating magnetic fields, but the fixed point dipole approximation is oversimplified and can readily be improved upon.

J. Self-consistent point dipoles

We have heretofore assumed that each particle is polarized only by the applied field. In reality, each particle also feels the field generated by all of the other dipoles in the suspension. These dipoles can be broken into two classes; those within the same chain and those in other chains. The dipole fields in other chains can be treated by the standard considerations of Lorentz cavity fields and demagnetizing fields, both of which depend on the concentration of particles. These effects have been examined in detail in magnetic studies of particle chain composites[10] and are only significant when the particle concentration approaches ∼5 vol. %. The experiments we investigate here were done at particle concentrations vastly lower than this, so we will ignore these fields. The fields created by particles in the same chain are not negligible, and here we will examine this effect, following the shear flow treatment of Martin and Anderson.[11]

The attractive dipole interaction between two contacting particles well in the interior of a long chain has been shown to be

$$\mathbf{f}_d = f_c \zeta(3)[(3\kappa_1 \cos^2\theta - \kappa_2)\hat{\mathbf{r}} + \kappa_3 \sin 2\theta\,\hat{\boldsymbol{\theta}}], \qquad (13)$$

where $\kappa_1 = (1 + \frac{1}{8}\xi^2)/(1 - \frac{1}{4}\xi - \frac{1}{8}\xi^2)^2$, $\kappa_2 = 1/(1 + \frac{1}{4}\xi)^2$, and $\kappa_3 = 1(1 - \frac{1}{4}\xi - \frac{1}{8}\xi^2)$, in terms of $\xi = \beta\zeta(3)$. The Rieman zeta function $\zeta(3) \sim 1.202$. The angle of a linear chain is given by a modified Eq. (7),

$$\sin 2\theta = \frac{16MnN^2}{\kappa_3 s(3)}. \qquad (14)$$

The chain will fracture when the radial component of the dipole force vanishes or $\cos\theta_c = \sqrt{\kappa_2/3\kappa_1}$.

Once again, we see that chain stability and metastability can be important in rotating fields, because the critical angle θ_c can range from 42.7° to 77.8° as β increases through its physical range of from $-1/2$ to $+1$ and thus is typically greater than 45°, where the tangential dipolar force reaches a maximum. Only in the interval of $-0.5 < \beta < -0.4$ does a metastable region not exist. The length of a critical chain is obtained from $\sin(2\theta_c) = 16MnN^2/\kappa_3 s(3)$. Noting that $\sin(2\theta) = 2\cos(\theta)\sqrt{1 - \cos^2\theta}$ gives

$$(2N^*)^2 = \frac{1}{2Mn} s(3)\kappa_3 \sqrt{\frac{\kappa_2}{3\kappa_1}\left(\frac{\kappa_2}{3\kappa_1}\right)}. \qquad (15)$$

Because in a real experiment the lifetimes of metastable chains might be quite long, it could be more relevant to consider the length of a chain at the limit of metastability, 45° for $\beta > -0.4$. Then $(2N^{**})^2 = (1/4Mn)s(3)\kappa_3$.

These approximate results for a linear chain imply that, depending on the contrast factor β, chains can fragment through brittle or ductile failure. Brittle failure is the abrupt fragmentation of a chain whose critical angle is less than 45°. Imagine, for example, an isolated chain of particles in a rotating field of very slowly increasing Mason number. As the Mason number increases, the chain will tilt further and further, always remaining quasistationary, until the critical Mason number is very slightly exceeded, at which point it will break abruptly. Chains with critical angles greater than 45° will behave very differently. As the Mason number increases, the chain will remain quasistationary until the angle 45° is attained. A slightly further increase in the Mason number will then cause the chain to continuously rotate to its critical angle and break. This is ductile failure.

K. Additional complexities

The remaining issues are the effect of hydrodynamic interactions and multipolar interactions. The primary effect of hydrodynamic interactions is to make the hydrodynamic drag twice as large when the fluid velocity is perpendicular to the rod as when it is parallel. In either case the drag coefficient is no longer strictly proportional to the chain length, since there is also an annoying logarithmic term. Despite this, the effect of hydrodynamic interactions on a linear chain in a rotating field is simple, since the chain friction, at least in the linear chain approximation, is always normal to the chain axis. The hydrodynamic interactions merely renormalize the drag and thus can be accounted for by renormalizing the Mason number, the critical chain angle remaining unchanged. (In this regard the simple shear case is more complex,[11] the critical chain angle changing because both the parallel and perpendicular drag coefficients enter.) Multipolar interactions[11] are not important for extant studies of chains in a rotating field, because of the low permeability of the magnetite-filled polystyrene particles employed.
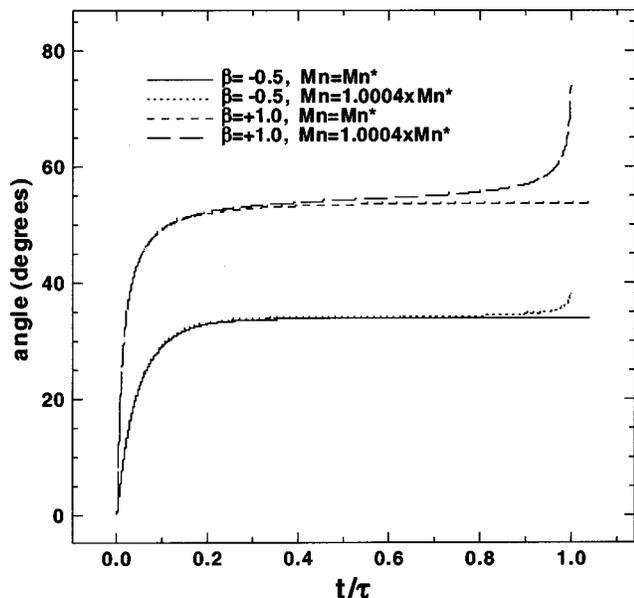
FIG. 4. Simulations of the dynamics of chain fragmentation are explored in the limits of extremely negative and positive permeability contrast. In the former case fragmentation is abrupt, in the latter gradual, justifying the concepts of brittle and ductile failure. The data are plotted only until the central chain particles part, and data for the fragmenting chains are compared to that of stationary chains.

III. SIMULATION AND EXPERIMENT

A. Simulation

In computer simulations one can simultaneously account for both the nonlinear chain shape and the self-consistent local fields, without any simplifying approximations. This enables us to determine whether such concepts as brittle or ductile chain failure are physically relevant. In the simulation we wrote, the spheres are essentially hard and feel a Stokes drag against the fluid. The dipole moments are computed completely self-consistently, without truncation of the dipole fields.

Using chains of 30 particles, the two extreme cases $\beta=-0.5$ and $\beta=+1.0$ were studied. In each case, the Mason number Mn^{**} that marks the limit of a stationary chain was found by noting that for larger Mn the chain fragmentation time τ diverges as an inverse power of $|Mn^{**}-Mn|$, analogous to critical slowing down in a second-order phase transition. Mn^{**} was found by choosing the value that gave the best power-law critical plot (a straight line plot of τ versus $|Mn^{**}-Mn|$ on log–log axes). Significantly Mn^{**} is more than 10 times larger for $\beta=+1.0$ than for $\beta=-0.5$, underlining the importance of positive contrast particles in making strong ER and MR fluids. Then in each case a simulation was conducted with a Mason number 0.04% larger than Mn^{**}, to ensure chain fracture. The simulation was stopped at the point of fracture.

The simulation result, Fig. 4, show some interesting features. First, with $\beta=-0.5$ the maximum angle for a stationary chain is $\sim 33.8°$, whereas with $\beta=+1.0$ this maximum angle is $\sim 53.6°$. Second, brittle failure is indeed observed for $\beta=-0.5$, occurring rapidly and with little change in angle before the two halves part. Progressive, ductile failure
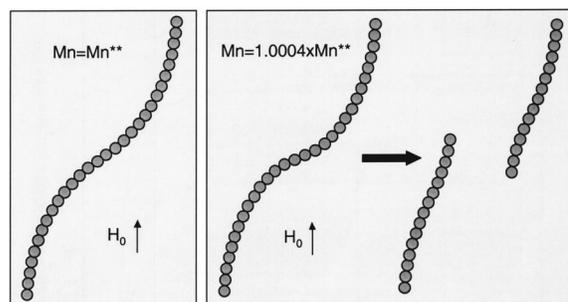

FIG. 5. In the case of ductile failure ($\beta=+1$) simulated structures are shown for a stationary chain at Mn^{**} (left) and a chain just before and after fragmentation (right). It is clear that the stationary chain configuration is easily distinguishable from that of the chain at the point of rupture.

is observed for $\beta=+1.0$, with a significant increase in the chain angle at rupture, up to $\sim 73.8°$. The actual chain configuration is shown in Fig. 5. The left image is a chain at Mn^{**}, showing the maximum deformation a stationary chain can achieve. The right image shows the deformation of a chain just before and just after rupture. These configurations are in the rotating reference frame of the applied field, so it is clear that the chain fragments are much more closely aligned with the field. In fact, the right-hand image is part of a closed dynamical cycle: after rupture the two chains orbit each other and reconnect to form a chain with swapped ends, which again deforms and breaks, etc.

B. Experiment

Videomicroscopy experiments[3] have shown that chains aggregate and fragment in response to decreasing or increasing field frequency, the average chain length being proportional to the inverse square root of Mn, in agreement with the predictions of this model. Videomicroscopy images[5] also confirm the prediction of the S shape developed by a critical chain in a counterclockwise rotating field, Fig. 6. These chains formed in an aqueous dispersion of 1.24 μm diameter soft magnetic particles having a volume fraction $\phi=0.0001$. The magnetic field amplitude was 1.55 kA/m (19.50 Oe), and the rotation frequency was 0.01 Hz. Chain fragmentation occurs in the following stages: the chain deforms slightly (left), develops a clearer S shape whose ends are aligned with the field (center), and breaks at the center into two equal fragments (right), which then align more closely with the field.

FIG. 6. Detail of the S shape developed by a critical chain in a counterclockwise rotating field of amplitude 1.55 kA/m (19.5 Oe) and frequency 0.01 Hz. These chains formed in an aqueous dispersion of 1.24-mm-diam soft magnetic particles at volume fraction 0.001.

IV. CONCLUSIONS

We have seen that the behavior of a chain in a rotating magnetic field is similar to the behavior of a chain in simple shear, but with some important conceptual and practical differences. First, the problem of a chain in a rotating field is in some ways subtle, since the curvature of the chain has a rather substantial effect on the critical chain angle, whereas this is not the case in simple shear. Second, rather substantial chain interference can occur, except at extremely low particle volume fractions, depending on the Mason number. Third, we have shown that a metastable regime exists and that this leads to the possibility of ductile fracture of a chain. Ductile fracture is shown to occur in simulations and in experiment. Similarities to the simple shear case include the finding that the critical chain length scales with the inverse square root of Mn and that its orientation relative to the instantaneous field is independent of Mn. Also, the nonlinear shape of a chain in a rotating field is actually quite similar to that in simple shear. In the future, detailed video microscopy studies should enable quantitative comparison of experiment to theory.

ACKNOWLEDGMENTS

[1] S. Melle, G. G. Fuller, and M. A. Rubio, Phys. Rev. E **61**, 4111 (2000).

[2] S. Melle, M. A. Rubio, and G. G. Fuller, Int. J. Mod. Phys. B **15**, 758 (2001).

[3] S. Melle, O. G. Calderón, M. A. Rubio, and G. G. Fuller, J. Non-Newtonian Fluid Mech. **102**, 135 (2002).

[4] S. Melle, O. G. Calderón, G. G. Fuller, and M. A. Rubio J. Colloid Interface Sci. **247**, 200 (2002).

[5] S. Melle, O. G. Calderón, M. A. Rubio, and G. G. Fuller, Int. J. Mod. Phys. B **16**, 2293 (2002).

[6] G. Helgesen, P. Pieranski, and A. T. Skjeltorp, Phys. Rev. Lett. **64**, 1425 (1990).

[7] G. Helgesen, P. Pieranski, and A. T. Skjeltorp, Phys. Rev. A **42**, 7271 (1990).

[8] T. C. Halsey, R. A. Anderson, and J. E. Martin, Int. J. Mod. Phys. B **10**, 3019 (1996).

[9] J. E. Martin, R. A. Anderson, and C. P. Tigges, J. Chem. Phys. **108**, 7887 (1998); **110**, 4854 (1999).

[10] J. E. Martin, E. Venturini, J. Odinek, and R. A. Anderson, Phys. Rev. E **61**, 2818 (2000).

[11] J. E. Martin and R. A. Anderson, J. Chem. Phys. **104**, 4814 (1996).

[12] J. A. Osburn, Phys. Rev. **67**, 351 (1946).

[13] T. B. Jones, *Electrodynamics of Particles* (Cambridge University Press, Oxford, 1995).

[14] A. P. Gast and C. F. Zukoski, Adv. Colloid Interface Sci. **30**, 153 (1989).

[15] O. Volkova, S. Cutillas, and G. Bossis, Phys. Rev. Lett. **82**, 233 (1999).

[16] J. Takimoto, H. Takeda, Y. Masubuchi, and K. Koyama, Int. J. Mod. Phys. B **13**, 2028 (1999).

[17] O. Volkova, G. Bossis, M. Guyot, V. Bashtovoi, and A. Reks, J. Rheol. **44**, 91 (2000).

[18] R. A. Anderson, in *Electrorheolocial Fluids: Mechanics, Properties, Structure, Technology, and Applications*, edited by R. Tao (World Scientific, Singapore, 1992), pp. 81–90.

[19] J. E. Martin, Phys. Rev. E **63**, 114061 (2001).